Available online at www.sciencedirect.com

ScienceDirect

Procedia CIRP 92 (2020) 100–105

www.elsevier.com/locate/procedia

16th CIRP Conference on Computer Aided Tolerancing (CIRP CAT 2020)

Comparison between two numerical tools for geometrical deviation analysis in composite assemblies

Andrea Corrado[a], Wilma Polini[a]*, Giovanni Moroni[b]

[a]Department of Civil and Mechanical Engineering, Università degli Studi di Cassino e del Lazio Meridionale, via G. di Biasio 43, 03043 Cassino, Italy
[b]Mechanical Engineering Department, Politecnico di Milano, via La Masa 1, 20156 Milano, Italy

* Corresponding author. Tel.: +39-07762993679; fax: +39-0776-2993546. *E-mail address:* polini@unicas.it

Abstract

The present work compares two numerical tools suitable to predict the geometrical deviations of an assembly constituted by thin laminates in composite material. The first one is based on a virtual representation of both the manufacturing and the assembling processes, able to generate the variability meta-model for each component to be used in a skin-based approach to assess whether the parts produced are assembled and meet the functional requirements. The second one estimates the sensitivity matrix that connects the components' variations to the assembly's variations in the method of influence coefficients (MIC). They were experimentally verified on a case study.

Keywords: composite; virtual representation; tolerance analysis.

1. Introduction

Composite materials are widely used to have a high ratio between strength and weight. Actually, they are involved in many products requiring high dimensional and geometrical accuracy. However, the combined effect of anisotropic characteristics of composite material, high temperature and high pressure to which the material is subjected during the cure process, arises residual stresses and, therefore, laminate deformations that involves many dimensional and geometrical defects [1,2].

Spring-in and warpage are the laminate deformations arising during cure process. Spring-in and warpage characterize curved and flat parts respectively. The first one is calculated as the difference between the measured and the theoretical value of the flange-to-flange angle at the end of the manufacturing process [3]. The second one is the curving of flat laminates, that produces a deviation from the original shape [3].

Distortions of composite laminates make difficult to assembly them. In fact, shimming operations are involved with an increase of costs and product weight, when no contact exists between the matching surfaces [4, 5]. This means that the gap formed by mating surfaces has to be filled by small sub-parts shaped according with the gap itself, since the high stiffness of the composite material makes difficult post-moulding repair/reshaping of the deformed shapes. Moreover, a high increase of the part internal stress may be involved by an assembly of deformed parts, thus deteriorating the part performance. This is a labour-intensive task, that extends the delivery time too.

Many studies of the literature were oriented to investigate the effects of the curing process and the residual stresses on a single component: the orthotropic behavior of the CTE at ply level may cause in-plane stresses that can give rise to distortion in unbalanced or unsymmetrical plates or else in non-planar laminates [6]. Chemical shrinkage produces laminate distortion too [7]. The resin flow causes a gradient on fiber volume fraction along the thickness, that influences the mechanical characteristic of the laminate and consequently it induces the warpage [8]. The greatest impact on the final shape of the laminate is imputable to the material interaction with the tool [9]. Some geometrical parameters together with structural

10.1016/j.procir.2020.05.190

parameters influence the spring-in angle of L-shaped parts [10,11].

The research works, on variation analysis of polymer matrix composite assemblies, are very few. An experimental approach to predict and control dimension variation for composites with polymer matrix and fiber reinforcement was used in [12]. The uncertainty in plies thickness and fiber orientations of polymer matrix composite materials and the spring-in phenomena due to the curing process was studied in [13].

In a previous work, the authors combined the spring-in deviations of L-shaped parts into a T-shaped assembly in polymer matrix reinforced by fibers through the method of influence coefficients [14-17] or by means of finite element analysis (FEA) [18]. It can be underlined that there is no work of the literature on the management of the entire information flow from manufacturing to assembly.

The present work compares two numerical tools suitable to predict the geometrical deviations of an assembly constituted by thin laminates in composite material. The first one is based on a virtual representation of both the manufacturing and the assemble processes, able to generate the variability meta-model for each component to be used in a skin-based approach to assess whether the parts produced are assembled and meet the functional requirements. It manages the entire information flow from manufacturing to assembly. The second one estimates the sensitivity matrix that connects the components' variations to the assembly's variations by the method of influence coefficients (MIC). The two tools were experimentally verified on a case study constituted by a T-shaped assembly made up of three parts. This is a type of structure commonly used in the design of components in composite material. All parts are joined by adhesive and their surfaces present warpage. Some L-shaped and flat parts were produced and, then, measured to evaluate their deviations in terms of warpage and spring-in. Those measured geometrical distortions were given as input to the numerical models.

The structure of this work foresees: in Section 2, the description of the two numerical tools to predict the geometrical deviations of an assembly is discussed. In section 3, the application of the two numerical tools to a T-shaped assembly is described. In section 4, all the obtained numerical results were compared to each other and with experimental tests and their differences are discussed. Finally, the conclusions are presented.

2. Numerical tools

In this section the two proposed numerical tools to manage the geometrical deviation analysis in composite assembly are introduced.

2.1. Virtual numerical model

The virtual numerical model manages the geometrical deviations from manufacturing to assembly for compliant parts in composite material virtually. It is based on a simulation tool and a skin model to represent the process signature, i.e. the pattern left by the process on the part surfaces. The skin model manages a set of points for each part boundary surface that are modified to represent the applied geometrical deviations [19]. In this work, the CaUTA software tool is used to generate the geometrical deviations of components to be assembled due to the variation of process parameters of the manufacturing process [18].

The developed tool is constituted by two parts: one for the manufacturing process (blue path in Fig. 1) and the other for the assembly process (orange path in Fig. 1). The first simulates a specific physical manufacturing process on the basis of a thermo-chemical model for curing process based on an energy balance:

$$\rho_c c_{p,c} \frac{\partial T}{\partial t} = \Delta\left(k_c \nabla t\right) + \rho_r V_r \dot{Q} \tag{1}$$

and a thermo-mechanical model with the aim of generating the geometrical deviations of the produced components in composite material due to the variation of process parameters, such as ply thickness, temperature and fiber orientation. In Eq.(1), ρ is the material density, c_p is the specific heat, T is the temperature, t is the time, k is the thermal conductivity coefficient of the composite material, $\dot{Q}$is heat generation rate of chemical reaction, V is the volumetric percentage, c and r refer to composite and matrix respectively.

This first part is used to generate the variability meta-model of each assembly component, once it was experimentally verified with production data:

$$\{W\} = \{W_n\} + \frac{\exp\left(-\frac{1}{2}\left(\{d\}-\{\mu\}\right)^T [\Sigma]^{-1}\left(\{d\}-\{\mu\}\right)\right)}{\sqrt{(2\pi)^k \|[\Sigma]\|}} \tag{2}$$

where $\{W\}$ is the vector of the node coordinates of the skin model shape $[X_1,\ldots,X_N,Y_1,\ldots,Y_N,Z_1,\ldots,Z_N]$ with N equals to the node number, $\{W_n\}$ is the vector of the node nominal coordinates, $\{d\}$ is the vector of the node deviations, $\{\mu\}$ and $[\Sigma]$ are the estimated mean vector and the covariance matrix of the multivariate normal probability density function. Therefore, this meta-model is used to generate the different part geometries that can be manufactured by the considered process, instead of producing and measuring a set of components, by reducing drastically the time to estimate the variability of a manufactured component in comparison with an experimental approach.

The second part of this simulation tool is constituted by a structural analysis that evaluates the variability of the assembly process starting from the variability meta-models of all the components. The analysis is based on the following relation:

$$\{u\} = \left[K_a\right]^{-1} \cdot \{F\} \tag{3}$$

since the assembly has a stiffness $[K_a]$, and a force vector $\{F\}$ generates a displacement vector $\{u\}$. The manufacturing signature, described in Eq. (2), is used to generate, the field of reaction forces that gave rise to the parts' deviations during the manufacturing process:

$$\{F\} = [K_u] \cdot \{W\} \tag{4}$$

with the subscripts a and u refer to assembly and parts stiffness matrix respectively.

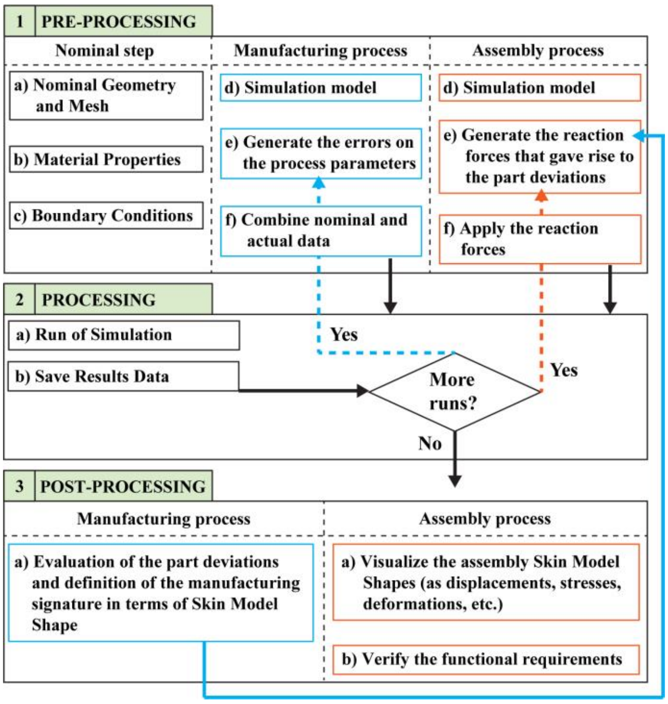

Fig. 1. Virtual numerical model.

The architecture of this virtual model is based on general-purpose software packages, such as MSC Marc® solver and Matlab® environment. FEA software discretizes the part features, interacts with the skin model to manage the geometrical deviations of the discretized features and combines them. Moreover, it may deal with contacts between the bodies, stress, deformation, displacement, contact quality and so on.

2.2. MIC numerical model

The MIC numerical tool is formed by four steps, as shown in Fig. 2. The first step models the geometrical deviations of the assembly parts depending on the manufacturing process with which the parts are obtained by means of the mean vector $\{\mu_p\}$ and the covariance matrix $[\Sigma_p]$ of the parts deviations estimated through experimental tests. The second step uses finite element analysis to evaluate stiffness of parts by taking as inputs the nominal part geometry and material properties. The third step takes into account the assembly sequence and the fastening operation by means of glue among the parts to evaluate the sensitivity matrix. The fourth step statistically estimates the assembly deviations, in terms of mean $\{\mu_a\}$ and covariance $[\Sigma_a]$, by the following equations:

$$\{\mu_a\} = [S] \cdot \{\mu_p\} \tag{5}$$

$$[\Sigma_a] = [S] \cdot [\Sigma_p] \cdot [S]^T \tag{6}$$

where $[S]$ is the sensitivity matrix.

This tool is developed in Matlab® environment that interacts with the MSC Marc solver that evaluates the stiffness matrices. All the details of the model are reported in [14].

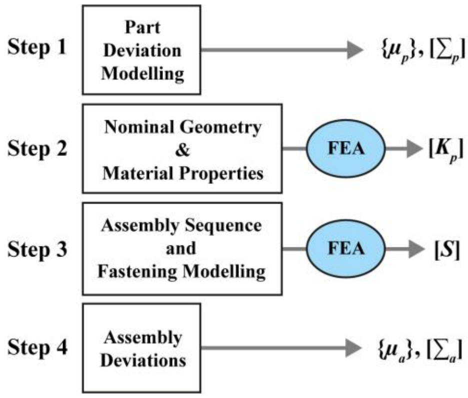

Fig. 2. MIC numerical model.

3. Comparison on the same application example

To compare the two numerical tools a T-shaped assembly was taken into account; it is formed by two L-shaped parts and one flat part (see Fig. 3) in composite material.

The parts were made of a unidirectional carbon-epoxy prepreg produced by Cytec with a designation of Cycom970/T300. This material was polymerized by means of vacuum bagging process. The parts were glued through a structural epoxy adhesive, Adekit A140 made by Axson®.

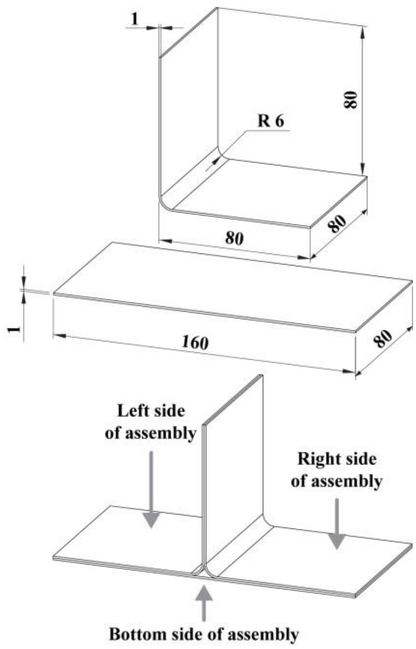

Fig. 3. T-shaped assembly (dimensions in mm).

3.1. Virtual numerical model

The virtual numerical model to represent the manufacturing process takes into account six prepreg plies laid on a U-shaped mould in aluminium with a $[0°,90°,0°]_s$ lay-up sequence. It uses a 3D mesh, constituted by brick elements (element number 149). The L-shaped and flat laminates were discretized by 1836 and 1683 nodes respectively. A Gaussian probability density function with a mean value equal to the nominal orientation value of the ply (0° or 90°) and a standard deviation of 0.85° and 0.01° for the manufacturing of L-shaped and flat laminates respectively was used to vary the ply orientation. Once defined the orientation of each ply, the nominal coordinates of the part nodes were re-generated with the new values representing the deviations from nominal due to the manufacturing process [20].

This first part of virtual representation was used to find the manufacturing signature for the two kinds of laminates, in terms of the multivariate probability density function of the deviations of the nodes from the nominal along the three axes x, y and z. The resulting deviation of each mesh node was evaluated through the square root of the sum of the squares of the three deviations along the three axes. These results were obtained by using the Monte Carlo method, where 800 and 1,000 iterations were run in order to simulate so many stacking of prepreg plies and to evaluate so many values of angles and flatness on L-shaped and flat laminates respectively that can be described by a mean value and a standard deviation [20].

The virtual representation of the assembly process estimates the variation of the assembly due to the two L-shaped parts and the flat part. It takes as input the instances of the variation meta-model belonging to the two laminates. This means that it transfers the field of forces $\{F_i\}$, with i=1 to 5355 nodes, associated with the geometrical deviations of the laminates. All parts are kept together by a glue thickness of 0.1 mm. The glue was discretized by means of 3D elements (element number 7) whose mechanical properties referred to Adekit A140. 500 simulation runs were carried out and the deviation from the nominal of the nodes constituting the assembly product along the three axes x, y and z were obtained [20]. The Euclidean norm was used to plot the assembly results in terms of mean deviation (a) and standard deviation (b), as shown in Fig. 4.

3.2. MIC numerical model

The T-shaped assembly was modelled by a mapped meshing with a total number of nodes and shell elements (element number 75) equal to 1751 and 1600 respectively.

Each of the two flat part surfaces was represented by a matrix 403x6, while each of the four L-shaped part surfaces was identified by a matrix 169x6. Each matrix was statistically elaborated to find the vector of the mean deviations and the covariance matrix [14].

To evaluate the stiffness matrix, a unit force, whose direction is that of variation, was applied at the i^{th} node of geometry where there is a variation (i = 1 to 1079). FEA calculated the displacement under the i^{th} unit force in the 1079 nodes interested by geometry variations (input). The stiffness matrix $[K_p]$ will be a 1079 x 1079 matrix with 1079 equal to the number of part variations that are the input of the tolerance analysis.

In the third step, FEA was used one more time to calculate the sensitivity matrix for the assembly. In this step, a point-to-point connection was used to simulate the glue [17,21], through beam-elements, in all areas of assembly between all nodes of parts. By this fastening modelling, no type of contact between parts to be assembled was used. The beam elements had a solid square cross-section with a side of 5 mm and a height of 0.1 mm, whose mechanical properties referred to Adekit A140. 884 beam elements were created (element number 98).

Finally, the Euclidean norm was used to plot the assembly results in terms of mean deviation (a) and standard deviation (b), as shown in Fig. 5.

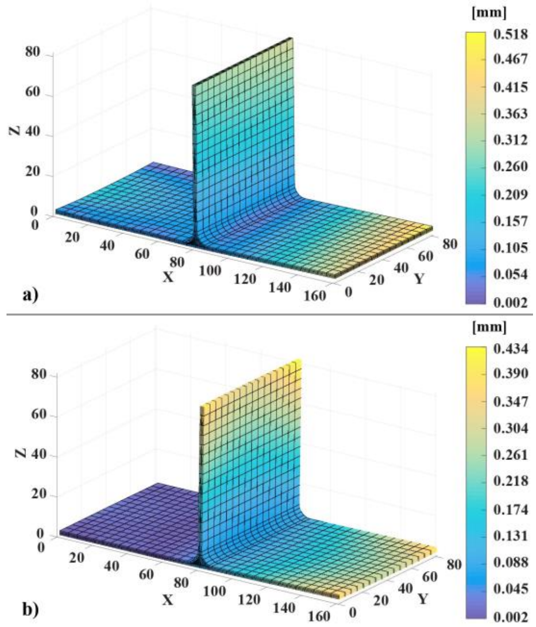

Fig. 4. a) Mean deviation and b) Standard deviation of the assembly deviations).

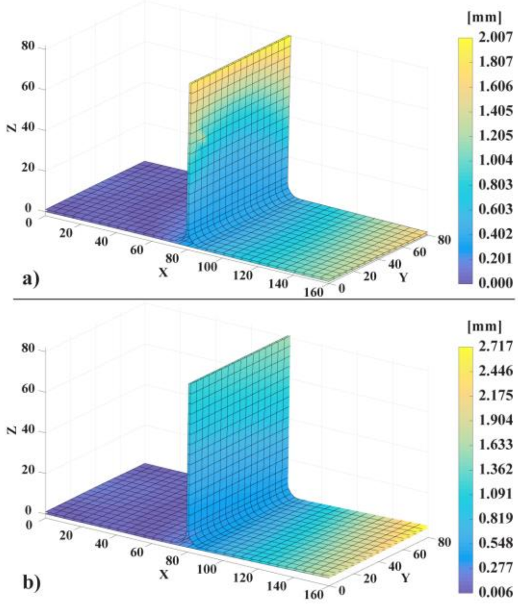

Fig. 5. a) Mean deviation and b) Standard deviation of the assembly deviations due to MIC model.

4. Results discussion

The obtained results of the angle values on the left and right sides of the T-shaped assembly together with the flatness of the bottom side of the same assembly are shown in the first four columns of Table 1 in terms of mean value and standard deviation for both the numerical tools. To evaluate the equality of variances and means respectively between the data due to the two numerical tools the Levene's and the Student's tests were used [22]. The results are reported in the first four columns of Table 2. They show that the mean and the variance values are statistically different, because the p-values of the test are lower than 0.05, except for the mean values of the right angle.

Moreover, some experimental tests were carried out to verify both the developed numerical tools. Six flat and twelve L-shaped laminates were manufactured by hand laying-up of prepreg on a U-shaped mould in aluminium. A vacuum of -10^5 Pa was applied after laying up the parts, in order to remove entrapped air and to minimize the possible effect of corner bridging. Then, the cure cycle began by heating the parts up to 140°C at 2.5°C/min. Once manufactured, the mould was left to cool down up to the room temperature before the composite parts were removed from the mould.

A Prismo Vast MPS coordinate measuring machine (CMM) of Zeiss® was utilized to measure the geometrical deviations of the manufactured part. The two kind of laminates were fixed to the U-shaped mould through standard trading components and modular elements. The mould was arranged by tapered clamps, that are clamping elements, on the granite plane of CMM; a probe with a tip diameter of 3 mm and a stylus length of 40 mm was used to measure spatial data. 169 points, i.e. 13-points along 13 lines, were acquired on each surface of each L-shape laminate; they were equally spaced at 5 mm. 403 points, i.e. 31-points along 13 lines, were measured on the two surfaces of each flat laminate; they were equally spaced at 5 mm.

Then, the components were glued through the structural epoxy adhesive Adekit A140 of Axson® in order to obtain six T-shaped assemblies. Then, each T-shaped assembly was measured through the CMM and fixturing equipment previously used to inspect the laminates. 169 points, i.e. 13-points along 13 lines, that were equally spaced at 5 mm, were measured on each surface, except for the bottom surface that was measured through 403 points, i.e. 31-points along 13 lines, that were equally spaced at 5 mm.

The angle between the flanges of each L-shaped laminate was calculated as the angle opposite to the normal to the two planes obtained by least square method. The flatness of each flat laminate was estimated through the sum of the distances of the two farthest points from the plane obtained by the least square method, one on the upside and one on the downside. The experimental results are reported in the last two columns of Table 1.

The results, in the last eight columns of Table 2, show that the virtual model and the experimental tests agree in terms of angle and flatness variability (same variance and same means), because the p-values are greater than 0.05. The results of the MIC model are statistically different from those due to experimental tests in terms of both the variance and the mean. In particular, the MIC model widely overestimates the standard deviation in general and the flatness mean value too.

This is probably due to a not exactly right evaluation of the sensitivity matrix due to the difficult of modelling the glue between the parts. A further difference between the MIC and the virtual model is connected with the modelling of part deviations that the two methods used as input. In fact, MIC models the part deviations through the experimental measurements, while the virtual model simulates the manufacturing process of parts to obtain the part deviations.

Fig. 6 shows the boxplots of the numerical and experimental data for the left and right angles and for the flatness of the T-shaped assemblies, i.e. a graphical summary of data distribution that shows its shape, central tendency and variability. It is clear how the MIC model gives results much more dispersed than those due to the virtual model. The trends of virtual model results are very similar to those due to experimental tests.

Table 1. Experimental and numerical results.

	Virtual model		MIC model		Experimental tests	
Measurement	Mean	Standard deviation	Mean	Standard deviation	Mean	Standard deviation
Left side angle [°]	89.80	0.15	89.64	1.34	89.90	0.13
Right side angle [°]	90.14	0.07	90.19	0.71	90.00	0.09
Bottom side flatness [mm]	0.48	0.15	1.05	0.61	0.46	0.04

Table 2. Statistical tests.

	Virtual vs MIC model				Experiments vs virtual model				Experiments vs MIC model			
	Levene's test		Student's test		Levene's test		Student's test		Levene's test		Student's test	
Measurement	T-value	p-value	T-value	p-value	T-value	p-value	T-value	p-value	T-value	p-value	T-value	p-value
Left side angle [°]	1437.60	0.000	2.66	0.008	0.51	0.473	-1.91	0.114	18.62	0.000	3.28	0.003
Right side angle [°]	1181.59	0.000	-1.59	0.113	0.33	0.564	3.67	0.014	13.82	0.000	-3.86	0.002
Bottom side flatness [mm]	375.44	0.000	-20.08	0.000	4.67	0.031	1.49	0.187	7.41	0.007	-18.58	0.000

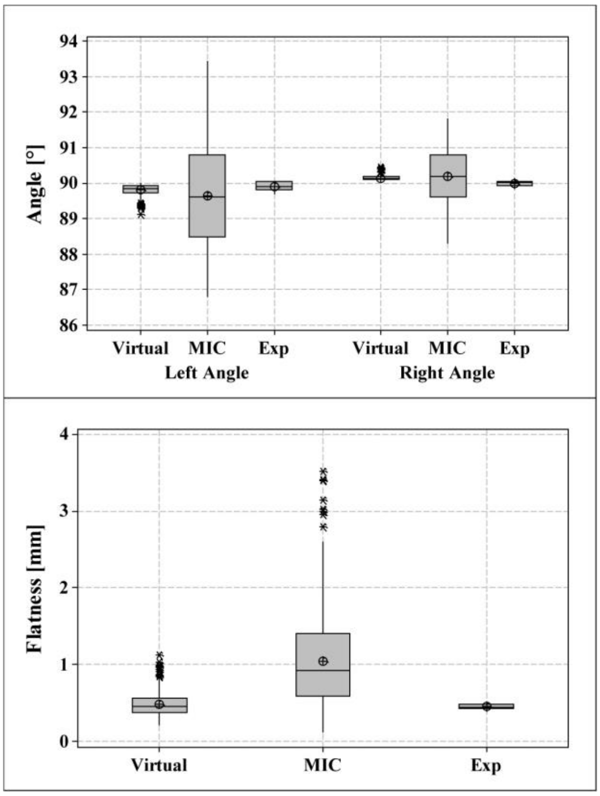

Fig. 6. Experimental and numerical results.

5. Conclusions

This work presents a comparison between two numerical tools for geometrical deviation analysis in composite assemblies. The first one, called virtual model since it manages virtually the geometrical deviations from manufacturing to assembly for compliant parts in composite material, may deal with linear and non-linear behaviors of the materials involved in all the process, it may deal with manufacturing signatures brought from every kind of process, it may involve every kind of geometry of the parts also very complex and it typically considers all the nodes of the parts. The second method does not present the previous advantages, for example it typically considers only the measured set of points on the parts, that is smaller than all the FEM nodes of the parts of the virtual model.

Those conclusions are verified by the comparison between numerical and experimental values that was carried out on the same application example. In fact, the virtual model carried out results near to experimental ones in terms of both mean value and standard deviation; this is verified by the statistical tests that were carried out. On the contrary, the results of the MIC model are statistically different from those due to experimental tests in terms of both the variance and the mean. In particular, the MIC model widely overestimates the standard deviation in general and the flatness mean value too. This depends to a not exactly right evaluation of the sensitivity matrix due to the difficult of modelling the glue between the parts, that is a current matter of study.

The time required by the virtual model to simulate the assembly was very similar to that due to the MIC approach for the considered case study by using a computer with an Intel core i7 950 processor running at 3.07 GHz, with 16 GB of RAM, a mechanical hard drive of 1TB at 5400 rpm, and running Windows 7 Professional.

Future works aim to improve the computational efficiency and to manage non-linear behaviors.

References

[1] Ding A, Li S, Wang J, Zu L. A three-dimensional thermo-viscoelastic analysis of process-induced residual stress in composite laminates. Compos Struct 2015;129:60–9.

[2] Tang S, Hu C. Design, Preparation and Properties of Carbon Fiber Reinforced Ultra-High Temperature Ceramic Composites for Aerospace Applications: A Review. J Mater Sci Technol. 2017;33:117–30.

[3] Albert C, Fernlund G. Spring-in and warpage of angled composite laminates. Compos Sci Technol. 2002;62:1895–912.

[4] Kappel E, Stefaniak D, Holzhüter D, Hühne C, Sinapius M. Manufacturing distortions of a CFRP box-structure – A semi-numerical prediction approach. Compos Part A Appl Sci Manuf 2013;51:89–98.

[5] Yang Y, Liu X, Wang YQ, Gao H, Bao Y, Li R. An enhanced spring-mass model for stiffness prediction in single-lap composite joints with considering assembly gap and gap shimming. Compos Struct 2018;187:18–26.

[6] Mahadik Y, Potter K. Experimental investigation into the thermoelastic spring-in of curved sandwich panels. Compos Part A Appl Sci Manuf 2013;4968–80.

[7] Baran I, Cinar K, Ersoy N, Akkerman R, Hattel JH. A Review on the Mechanical Modeling of Composite Manufacturing Processes. Arch Comput Methods Eng 2017;24:365–95.

[8] Sorrentino L, Esposito L, Bellini C. A new methodology to evaluate the influence of curing overheating on the mechanical properties of thick FRP laminates. Compos Part B Eng 2017;109:187–96.

[9] Kappel E. Forced-interaction and spring-in – Relevant initiators of process-induced distortions in composite manufacturing. Compos Struct 2016;140:217–29.

[10] Corrado, A., Polini, W., Moroni, G., Petrò, S. 2018, A variational model for 3D tolerance analysis with manufacturing signature and operating conditions, Ass Autom 2018;38:10-19.

[11] Corrado A, Polini W. Analysis of process-induced deformation on the spring-in of carbon fiber-reinforced polymer thin laminates. J Com Mater 2019;53:2901-2907.

[12] Dong C, Kang L. Deformation and stress of a composite–metal assembly. Int J Adv Manuf Techn 2012;61:1035–1042.

[13] Jareteg C, Wärmefjord K, Cromvik C, Söderberg R, Lindkvist L, Carlson JS, Larsson S, Edelvik F. Geometry assurance integrating process variatio with simulation of spring-in for composite parts and assemblies. J Comput Inf Sci 2016;16(3):031003.

[14] Corrado A, Polini W, Moroni G. Manufacturing signature and operating conditions in a variational model for tolerance analysis of rigid assemblies. Res Eng Des 2017;28:529-544.

[15] Polini W, Corrado A. Uncertainty in manufacturing of lightweight products in composite laminate: part 1 – numerical approach. Int J Adv Manu Tech 2019;101(5-8):1423-1434.

[16] Polini W, Corrado A. Uncertainty in manufacturing of lightweight products in composite laminate: part 2 – experimental validation. Int J Adv Manu Tech 2019;101(5-8):1391-1401.

[17] Variation analysis of compliant parts in composite material joined by adhesive: a numerical tool. Trans ASME J Manu Sci Eng 2019;140:094502.

[18] Corrado A, Polini W. A new way to solve tolerance analysis: the Cassino Unified Tolerance Analysis tool. Int J Comp Int Manu 2019;32:124–35.

[19] Anwer N, Ballu A, Mathieu L. The skin model, a comprehensive geometric model for engineering design. CIRP Ann Manu Tech 2013;62:143–6.

[20] Polini W, Corrado A. Digital twin of composite assembly manufacturing process. Accepted for publication on Int J Prod Res 2020.

[21] MSC Software. Marc – Volume A: Theory and User Information. 2013.

[22] Montgomery, D. C., G.C. Runger, and N.F. Hubele. 2011. "Engineering Statistics." John Wiley and Sons, Inc.